Electronic Supplementary Information

Isolated Fe atoms dispersed on cellulose-derived nanocarbons as efficient electrocatalyst for oxygen reduction reaction

Xiaofeng Li,[a] Yuhao Zhang, [a] Jinfang Zhang, [a] and Congwei Wang * [b]

[a] School of Materials Science and Engineering, North University of China, Taiyuan 030051, PR China

[b] CAS Key Laboratory of Carbon Materials, Institute of Coal Chemistry, Chinese Academy of Sciences, Taiyuan, 030001, P. R. China.

Email: wangcongwei@sxicc.ac.cn

Experiment Section

Chemicals.

Graphite (99.95% purity) was obtained from Qingdao Huarun Graphite Co., Ltd., Chemically pure ferric chloride ($FeCl_3$), cellulose powder (98 %), potassium hydroxide (KOH, 97 %), hydrochloric acid (HCl, 37 %) and urea were purchased from Sinopharm Chemical Reagent Co., Ltd. All aqueous solutions were prepared by deionized water. All chemicals were used without further purification.

Preparation of isolated Fe atoms dispersed on cellulose-derived nanocarbons (aFe-NGC)

The graphene was prepared using the established electrochemical approach. The preparation of isolated Fe atoms dispersed on cellulose-derived nanocarbons (aFe-NGC) is based on classic KOH chemical activation. Typically, 50 mL graphene dispersion (4mg mL^{-1}), 36 mL cellulose solution (0.1 g mL^{-1}), 35 mL urea solution (0.1 g mL^{-1}) and 10 mL $FeCl_3$ solution (0.2 mol L^{-1}) were mixed for 12 hours under ambient condition. Then 4 g KOH powder was added to the above dispersion with continuously stirring for 4 hours. After lyophilization, the obtained mixture solid was annealing at high temperature ranging from 550 to 750 ºC for 2 hours. The obtained annealed intermediate sample is denoted as FeOC-NGC. The acid and water leaching was then applied to annealed powder to wash away inactive metal oxides and impurities. The prepared catalyst, isolated Fe atoms dispersed on cellulose-derived nanocarbons, denoted as aFe-NGC, was dried at 60 ºC overnight before

electrocatalytic measurements. The same procedure was applied to make nitrogen doped graphene/nanocarbon, denoted as NGC.

Instrumental characterization.

The scanning electron microscopy (SEM) was conducted using JSM-7001F field emission SEM. Transmission electron microscopy (TEM) images were taken with JEM-2100F microscope at an acceleration voltage of 200 kV. Aberration-corrected scanning transmission electron microscopy (STEM) was performed on a JEM ARM200F equipped with double aberration correctors in Institute of physics, Chinese Academy of Sciences. High-angle annular dark field (HAADF) STEM images were recorded using a HAADF detector with a convergence angle of 25 mrad and a collection angle between 70 and 250 mrad. Under these conditions, the spatial resolution is ca. 0.08 nm. X-ray photoelectron spectroscopy (XPS) measurements were performed using Thermo ESCALAB 250 spectrometer, employing an Al-KR X-ray source with a 500 μm electron beam spot. Raman spectra were recorded using Jobin-Yvon HR-800 Raman system with 532 nm line of Ar laser as excitation source. The Brunauer−Emmett−Teller (BET) specific surface area were deduced from the N_2 physical adsorption measurement data that were obtained using an ASAP 2010 Accelerated Surface Area and Porosimetry System. XANES measurements at Fe K-edge in transmission mode were performed at the BL14W1 in Shanghai Synchrotron Radiation Facility. The electron beam energy was 3.5 GeV and the stored current was

230 mA (top-up). The raw data analysis was performed using IFEFFIT software package according to the standard data analysis procedures.

Electrochemical measurements.

The electrocatalytic performances were measured using a set of electrochemical methodologies, such as cyclic voltammetry (CV), rotating disk electrode (RDE) in a three-electrode electrochemical cell. The platinum wire and Ag/AgCl were used as the counter electrode and the reference electrode respectively. Autolab electrochemical analyser (PGSTAT204) and a MSR electrode rotator (PINE, US) were employed as the electrochemical station. The catalyst ink was prepared by mixing the catalyst (8 mg) with 2 ml ethanol-water (1:1) and 8 μL Nafion with the assistance of sonication. Subsequently, the catalyst was loaded on the surface of GC electrode surface (diameter: 5 mm) by drop casting and dried in air. It is noted that special care was taken to maintain the loading of the catalysts the same in all samples. All the experiments were conducted at room temperature, in an O_2 or N_2-saturated 0.1 M KOH aqueous solutions as electrolyte. All samples were tested for 5 times for the consistence and commercial Pt-C catalyst (20 wt. %) was used for comparison. CV curves were measured at a scan rate of 50 mv s^{-1} and LSV curves were at 10 mv s^{-1}. Chronoamperometric curves were tested at -0.3 V in O_2 saturated 0.1 M KOH at a rotation speed of 1200 rpm. The 3M concentration methanol solution was injected into the electrochemical cell at about 150 s for evaluating the reluctance to methanol poisoning.

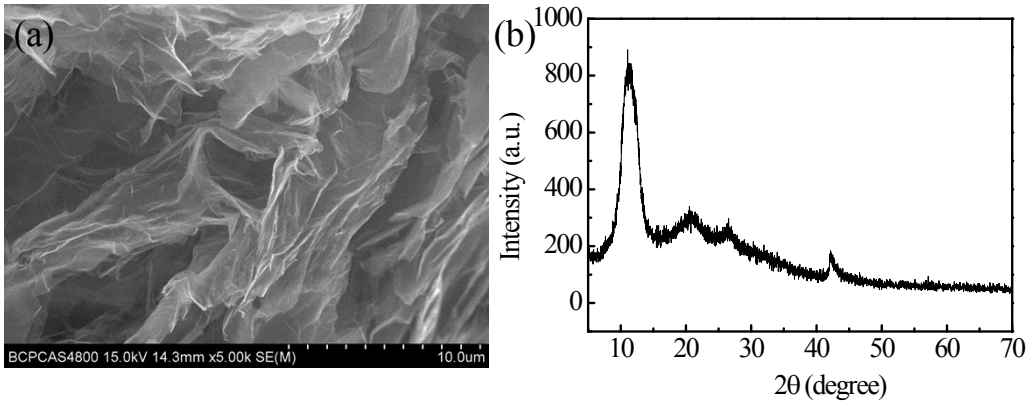

Fig. S1 (a) SEM image of electrochemically exfoliated raw graphene nanosheets, (b) XRD spectrum of raw graphene.

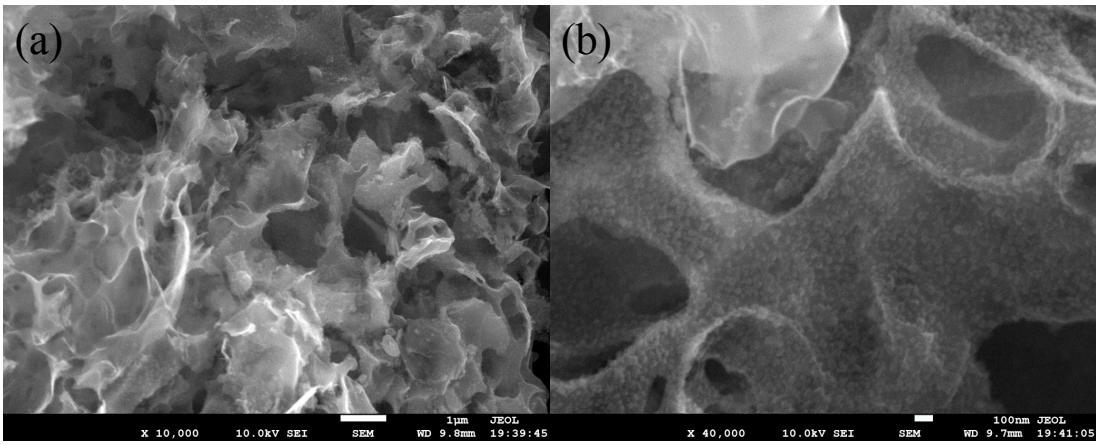

Fig. S2 SEM images of intermediate FeOC-NGC before acid/water leaching, in (a) low and (b) high magnifications.

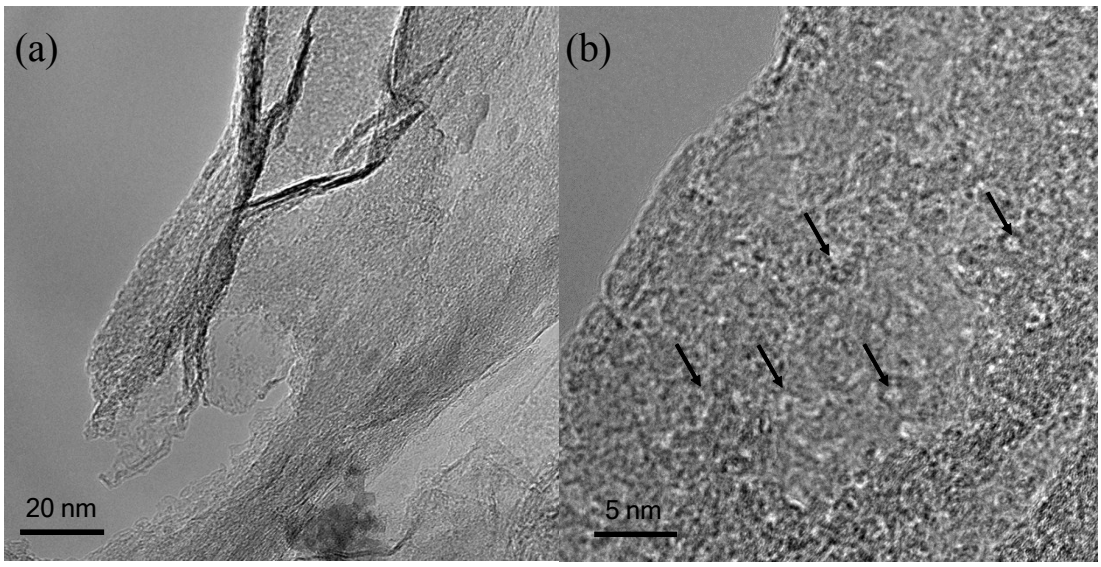

Fig. S3 TEM image of aFe-NGC catalyst after acid leaching, the arrow indicates the micropores generated via pyrolysis.

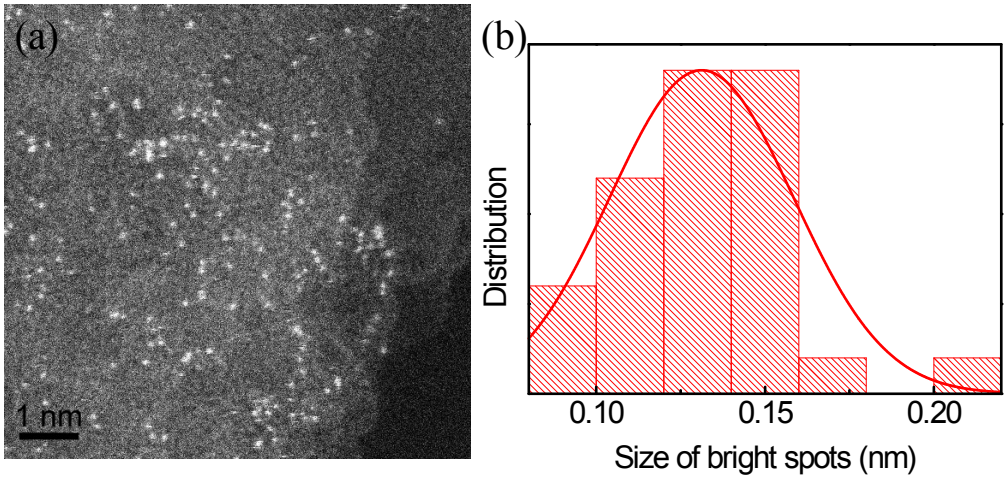

Fig. S4 (a) HRSTEM image of aFe-NGC and (b) the histogram of bright spots size distribution.

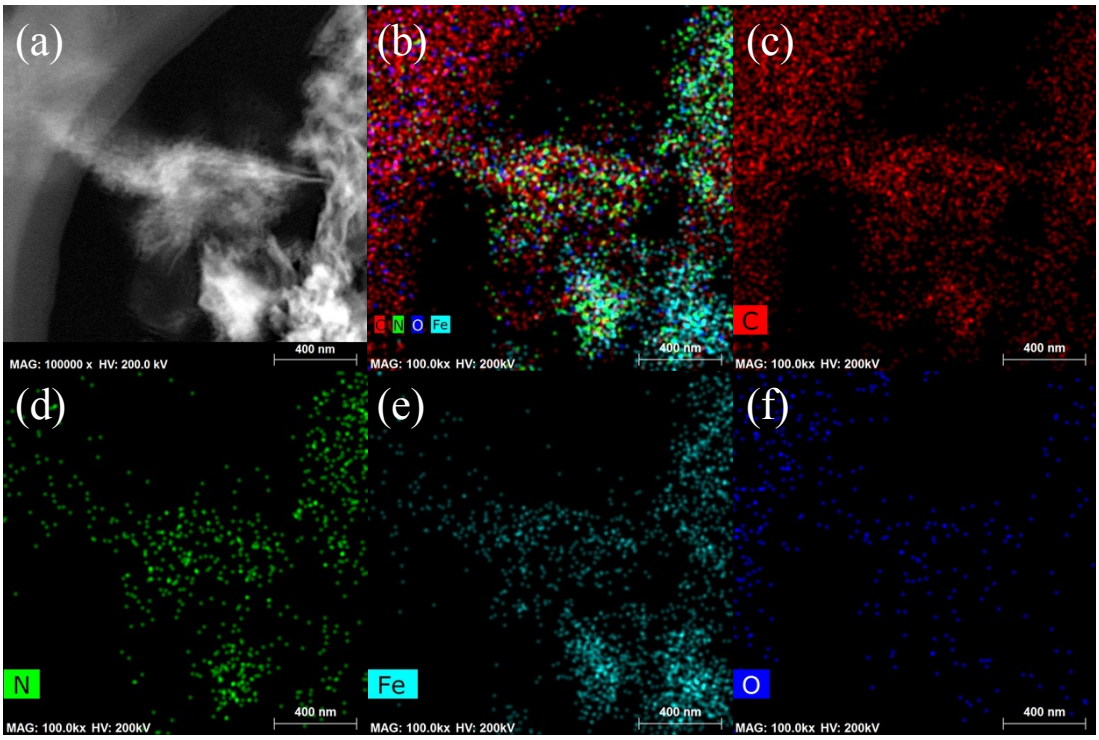

Fig. S5 (a) STEM image of aFe-NGC and corresponding element mapping of (b) overall elements and (c-f) C, N, Fe, O, respectively.

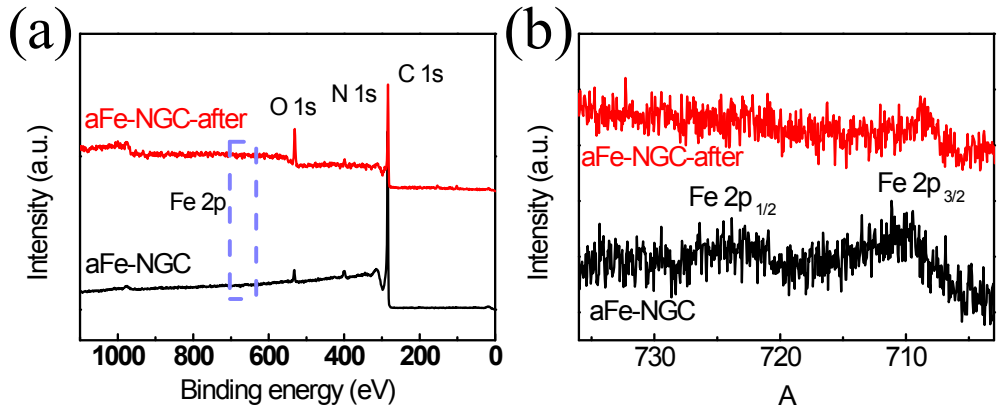

Fig. S6 (a) Long range spectrum of aFe-NGC (b) Fe 2p spectrum of aFe-NGC before and after the catalyst's stability measurement.

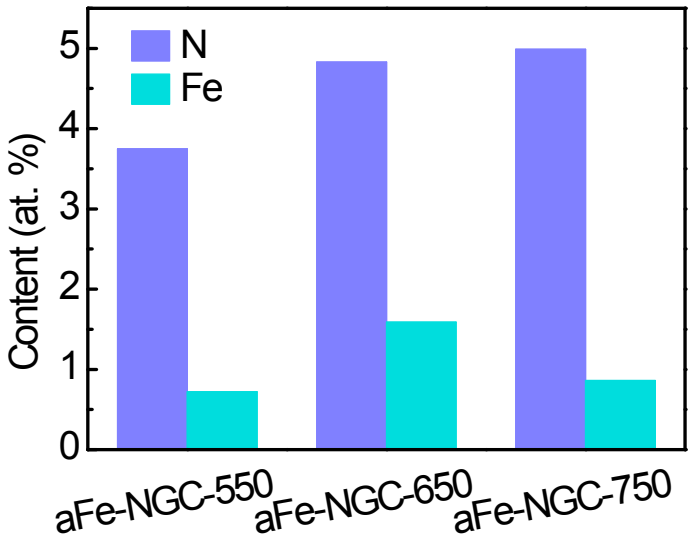

Fig. S7 Fe and N content for aFe-NGC obtained in different activation temperatures.

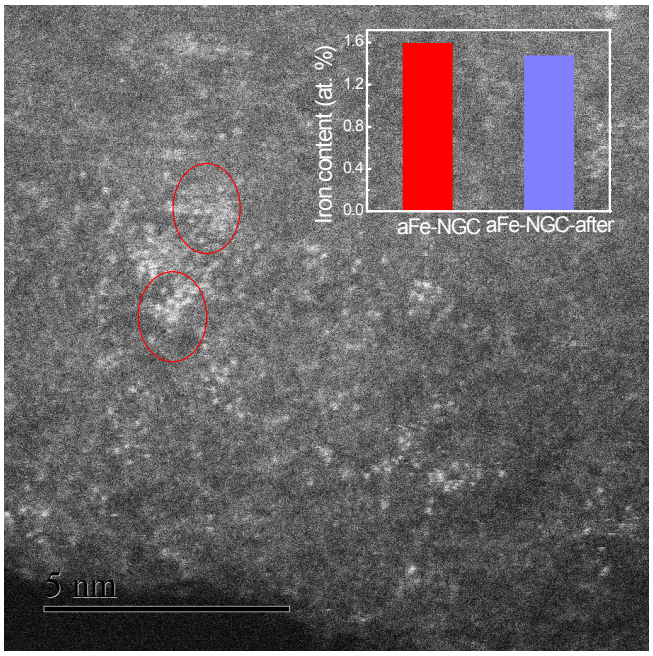

Fig. S8 HAADF-STEM image of aFe-NGC after catalyst's stability measurement, the inset shows the change of iron content in aFe-NGC.

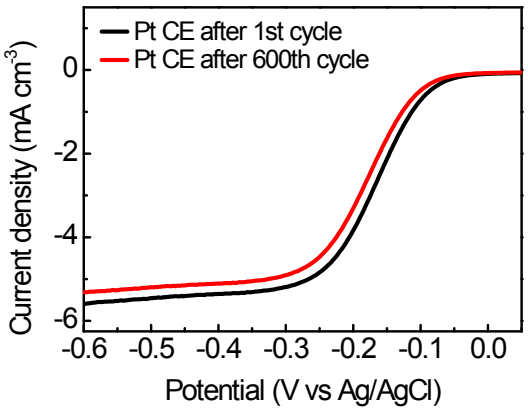

Fig. S9 LSV curves of aFe-NGC at 1600 rpm in 0.1 M KOH electrolyte after 1st and 600th cycles.

Table S1. A comparison for a range of SAC-Fe and Fe-N-C electrocatalysts and aFe-NGC in this work.

Materials	Loading (μg cm^{-2})	Onset potential (V *vs*. RHE)	Half-wave potential (V *vs*. RHE)	Ref
Fe-CNT-PA	500	0.93	0.80	S1
Fe-NMP, Fe-NMG	600	0.97	0.84	S2
COP@K10-Fe-900	200	0.97	0.85	S3
Fe-CB@PAN-1000	800	n. a.	0.88	S4
Fe_3C/NG-800	400	1.03	0.86	S5
EDC4	600	0.96	0.80	S6
Fe–N–GC-900	600	1.01	0.86	S7
Fe@BC-800	420	1.01	0.85	S8
Fe-NGM/C-Fe SAC	160	1.05	0.86	S9
Fe-ISAs/CN SAC	408	0.99	0.90	S10
Fe@C-FeNCs-2	700	1.00	0.90	S11
MF-Fe-800 SAC	400	0.98	0.83	S12
Fe_{SA}–N–C SAC	280	n. a.	0.89	S13
SA-Fe/NG SAC	240	0.90	0.80	S14
Fe SAs/MC SAC	200	1.03	0.90	S15

aFe-NGC	**160**	**0.97**	**0.83**	**This work**

References

[S1] Yang, G.; Choi, W.; Pu, X.; Yu, C. *Energy Environ. Sci.* **2015**, *8*, 1799.

[S2] Hossen, M. M.; Artyushkova, K.; Atanassov, P.; Serov, A. *J. Power Sources* **2018**, *375*, 214.

[S3] Guo, J.; Cheng, Y.; Xiang, Z. *ACS Sustainable Chem. Eng.* **2017**, *5*, 7871.

[S4] Chen, J. L.; Li, W. B.; Xu, B. Q. *J. Colloid Interface Sci*. **2017**, 502, 44.

[S5] Xiao, M. L.; Zhu, J. B.; Feng, L. G.; Liu, C. P.; Xing, W. *Adv. Mater.* **2015**, *27*, 2521.

[S6] Gokhale, R.; Chen, Y.; Serov, A.; Artyushkova, K.; Atanassov, P. *Electrochem. Commun.* **2016**, *72*, 140.

[S7] Kong, A.; Zhu, X.; Han, Z.; Yu, Y.; Zhang, Y.; Dong, B.; Shan, Y. *ACS Catal.* **2014**, *4*, 1793.

[S8] Ma, X.; Lei, Z.; Feng, W.; Ye, Y.; Feng, C. *Carbon* **2017**, 123, 481.

[S9] Wang, C.; Zhang, H.; Wang, J.; Zhao, Z.; Wang, J.; Zhang, Y.; Cheng, M.; Zhao, H.; Wang, J. *Chem. Mater.* **2017**, *29*, 9915.

[S10] Jiang, W. J.; Gu, L.; Li, L.; Zhang, Y.; Zhang, X.; Zhang, L. J.; Wan, L. J. *J. Am. Chem. Soc.* **2016**, *138*, 3570.

[S11] Chen, Y.; Ji, S.; Wang, Y.; Dong, J.; Chen, W.; Li, Z.; Li, Y. *Angew.Chem. Int. Ed.* **2017**, *56*, 6937.

[S12] Lu, B.; Smart, T. J.; Qin, D.; Lu, J. E.; Wang, N.; Chen, L.; Peng, Y.; Ping, Y.; Chen, S. *Chem. Mater.* **2017**, 29, 5617.

[S13] Jiao, L.; Wan, G.; Zhang, R.; Zhou, H.; Yu, S. H.; Jiang, H. L. *Angewandte Chemie*, **2018**, 130, 8661-8665.

[S14] Yang, L.; Cheng, D.; Xu, H.; Zeng, X.; Wan, X.; Shui, J.; Xiang, Z.; Cao, D. *Proc. Natl. Acad. Sci. U.S.A.*, **2018**, 201800771.

[S15] Yang, Z. K.; Yuan, C-Z.; Xu, A-W. *ACS Energy Lett.* 2018, 3, 10, 2383-2389